Scientific Research Publishing

World Journal of Engineering and Technology, 2025, 13(2), 225-233
https://www.scirp.org/journal/wjet
ISSN Online: 2331-4249
ISSN Print: 2331-4222

Research on C80 Train-Track Coupling Model

Lili Liu[1], Jihong Zuo[2], Yan Li[2], Chuanyin Yang[1], Qingwan Tang[1], Tianle Kuang[1]

[1]College of Intelligent Control, Hunan Railway Professional Technology College, Zhuzhou, China
[2]College of Rail Transit Locomotive and Rolling Stock, Hunan Railway Professional Technology College, Zhuzhou, China
Email: 277644902@qq.com

How to cite this paper: Liu, L.L., Zuo, J.H., Li, Y., Yang, C.Y., Tang, Q.W. and Kuang, T.L. (2025) Research on C80 Train-Track Coupling Model. *World Journal of Engineering and Technology*, **13**, 225-233.
https://doi.org/10.4236/wjet.2025.132014

Received: February 21, 2025
Accepted: March 24, 2025
Published: March 27, 2025

Abstract

It is difficult to express the mathematical relationship between the key parameters of suspension and the optimization objectives with intuitive mathematical expressions in the multi-body dynamics model of vehicle-track coupling, the RBFNN surrogate model between suspension key parameters and optimization objectives is built by MATLAB, and R^2 is used as an index to evaluate the accuracy of the surrogate model. By using the K-means Clustering Method, when the number of clusters is 400, the R^2 values of the training set and the prediction set are greater than 0.9, the results show that the fitting effect of the surrogate model is good, and the accuracy meets the requirements.

Keywords

Vehicle-Track Coupling, Suspension Parameters, Surrogate Model

1. Introduction

Because the vehicle-track coupling multi-body dynamics model involves many complex suspension parameters, which vary widely, the suspension parameters of the vehicle-track coupling multi-body dynamics model can not be ignored, it is difficult to accurately describe the complex mathematical relationship between suspension parameters and optimization objectives through intuitive mathematical expressions [1]. In order to solve this problem, the surrogate model is introduced. Firstly, the influence of different suspension parameters on the vibration of the car body is calculated by the Variable Importance in the Projetion (VIP) analysis method, the key parameters that have great influence on the vertical vibration acceleration and lateral acceleration of the car body are screened out, vertical and lateral surrogate models between key parameters and optimization objectives are constructed by radial basis function neural networks (RBFNN) based on the K-means clustering algorithm, which can be used to predict the perfor-

mance of the proposed model, the rationality of the surrogate model is verified by comparing the simulation results with the predicted values of the vertical and horizontal surrogate models.

2. System Description

The bogies for C80 freight cars are type K6, as shown in Figure 1.

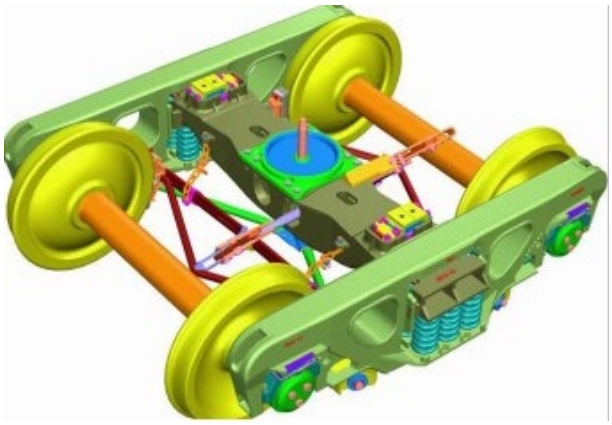

Figure 1. Schematic diagram of K 6 bogie.

The K6 bogie is the key component of the traditional freight car, its structural foundation covers several key parts: the wheel group, axle box suspension unit (using rubber pad), side beam, pillow spring suspension system, shock absorber unit, center pin, and constant contact elastic side bearing [2]. This complex structure contains a wealth of nonlinear dynamic characteristics, such as various clearance effects, the role of limiters, the impact of wedge damping, the friction torque between the center plate and the side bearing, these all have a significant impact on overall performance.

3. Determination of Key Suspension Parameters

As an important part of the locomotive, the parameters of the bogie suspension system directly affect the dynamic performance and ride comfort of the locomotive, there is a close relationship between the locomotive carbody vibration acceleration and the bogie suspension parameters, so the carbody vibration acceleration is used to measure the rationality of the suspension parameters. Based on the initial parameters of C80 heavy haul freight cars provided by a heavy haul railway, the range of dynamic suspension parameters is determined in combination with relevant experience. The specific parameters and their corresponding ranges are shown in Table 1.

Table 1. The variables of suspension parameters for heavy-load freight vehicles.

Serial number	Name of the suspension parameter	Unit	Range of sampling values
1	Longitudinal stiffness of rubber pad per axle box	MN/m	1 - 30

Continued

2	Lateral stiffness of rubber pad per axle box	MN/m	1 - 30
3	Vertical stiffness of each axle box rubber pad	MN/m	50 - 250
4	Longitudinal stiffness of secondary system	MN/m	0.5 - 20
5	Lateral stiffness of secondary system	MN/m	0.5 - 20
6	Vertical stiffness of secondary system	MN/m	0.5 - 20
7	Vertical stiffness of elastic side bearing	MN/m	0.5 - 20
8	Relative coefficient of friction of inclined wedge	/	0.05 - 0.3

The vibration acceleration data of the C80 freight car comes from the data collected by the vibration sensor. The vibration sensor is installed under the car body at the rear wheelset of the front bogie, and the vibration acceleration signals, including the lateral and vertical directions of the car body are collected, the sampling frequency is 100 Hz. According to GB5599-2019 "Specification for evaluation and test qualification of locomotive and vehicle dynamics performance", it is necessary to carry out band-pass filtering processing when analyzing vehicle vibration acceleration data. In this paper, the measured and simulated car body acceleration data are processed by 0.4 Hz - 40 Hz band-pass filter. The Pearson product-moment correlation coefficient between the simulated vehicle body vibration acceleration power spectral density after filtering and the measured vehicle body vibration acceleration power spectral density is calculated, and it is used as the evaluation index of the influence of suspension parameter change on carbody acceleration. The Pearson correlation function is calculated by formula (1)

$$\rho\left[x_s(\omega), x_f(\omega)\right] = \frac{1}{\sqrt{E\left[x_s(\omega)^2\right] - \left\{E\left[x_s(\omega)\right]\right\}^2}} \cdot \frac{E\left[x_s(\omega)x_f(\omega)\right] - E\left[x_s(\omega)\right]E\left[x_f(\omega)\right]}{\sqrt{E\left[x_f(\omega)^2\right] - \left\{E\left[x_f(\omega)\right]\right\}^2}} \tag{1}$$

Among them, $x_s(\omega)$ and $x_f(\omega)$ are the power spectral density functions of the simulated values and the measured values after band-pass filtering, respectively. $\rho[x_s(\omega), x_f(\omega)]$ represents the Pearson correlation coefficient between the power spectral density functions of the simulated values and the measured values. $E[\ ]$ represents the expected value of the sample.

Taking the 8 suspension parameters in Table 1 as the variables affecting the vibration acceleration of the car body, the variable VIP analysis method is adopted, the influence degree of the eight suspension parameters on the evaluation index of the dependent variable is calculated. The variable projection importance analysis method is a variable screening method based on the partial least squares algorithm. By calculating the projection contribution of each suspension parameter factor variable in the evaluation index, the variable projection importance analysis method is used to analyze the influence of each suspension parameter variable on the evaluation index, to evaluate the degree of interpretation

of the factor variable to the target variable. The existing conclusion holds that when $VIP_{im} > 1$, it indicates that the factor variable x_i is an important influencing factor of the dependent variable ρ_m.

Based on 1000 sets of different suspension parameters, the car body acceleration is simulated as the predicted value, and the car body acceleration based on the original vehicle parameters is the real value. The vertical and lateral accelerations ρ_{zs} and ρ_{ys} between the predicted values and the true values can be obtained from formula (1). Taking the eight suspension parameters in Table 1 as input variables, and ρ_{zs} and ρ_{ys} as output variables, the VIP values of the eight parameters for ρ_{zs} and ρ_{ys} are calculated. The calculation results are shown in Table 2.

Table 2. The VIP value corresponding to the suspension parameter.

Serial number	Name of the suspension parameter	The VIP value of ρ_{zs}	The VIP value of ρ_{ys}
1	Longitudinal stiffness of rubber pad per axle box	0.29	0.59
2	Lateral stiffness of rubber pad per axle box	0.32	0.55
3	Vertical stiffness of each axle box rubber pad	**1.71**	**1.23**
4	Longitudinal stiffness of secondary system	0.63	0.21
5	Lateral stiffness of secondary system	0.60	**1.86**
6	Vertical stiffness of secondary system	**2.12**	**1.35**
7	Vertical stiffness of elastic side bearing	**1.03**	0.47
8	Relative coefficient of friction of inclined wedge	0.52	**1.19**

As can be seen from Table 2, among the influencing factor variables of ρ_{zs}, the VIP values of the vertical stiffness of the rubber pad, the vertical stiffness of the secondary spring, and the vertical stiffness of the elastic side bearing are greater than 1. Therefore, these three factor variables are regarded as the key parameters for the vertical vibration acceleration of the vehicle body. Among the influencing factor variables of ρ_{ys}, the VIP values of the vertical stiffness of the rubber pad, the lateral stiffness of the secondary spring, the vertical stiffness of the secondary spring, and the relative friction coefficient of the inclined wedge are greater than 1. Therefore, these four factor variables are regarded as the key parameters for the lateral vibration acceleration of the vehicle body.

4. Construction of RBFNN Surrogate Model

The surrogate model can effectively capture the main characteristics of the original dynamic model and simplify the calculation process. At present, there are polynomial response surface (RSM) [3], Kriging model [4], radial basis function (RBF) [5], support vector machine (SVR) [6], polynomial chaos expansion (PCE) [7] and so on, in this paper, radial basis function neural network (RBFNN) is selected as the surrogate model of multibody dynamics.

As a neural computing model with single hidden layer architecture, radial basis function (RBF) neural network has concise structure and excellent nonlinear

mapping characteristics. The core strategy relies on the radial basis function (RBF) as the basic building block, skillfully uses the output information of the training sample, and generates the surrogate model by measuring the geometric distance between the point to be predicted and the sample point. This design strategy skillfully transforms high-dimensional complex problems into a single one-dimensional processing flow, greatly improving efficiency [8]. The mathematical expression of the radial basis function surrogate model is shown in (2)

$$f(x)=\sum_{i=1}^{n}\omega_i\phi\left(\left\|\boldsymbol{x}-\boldsymbol{u}_i\right\|\right)+b_0 \tag{2}$$

Among them, n represents the number of hidden layer neurons, ω_i represents the weight value, x represents the input parameter vector, u_i represents the center vector of hidden nodes in the hidden layer, b_0 represents the bias value, $\left\|\boldsymbol{x}-\boldsymbol{u}_i\right\|$ represents the Euclidean norm from the input vector to the center vector, indicating the distance between x and u_i, ϕ represents the Gaussian radial basis function, and its mathematical expression is shown as (3).

$$\phi\left(\left\|\boldsymbol{x}-\boldsymbol{u}_i\right\|\right)=\exp\left(-\frac{\left\|\boldsymbol{x}-\boldsymbol{u}_i\right\|^2}{2\sigma_i^2}\right) \tag{3}$$

Where σ_i is the normalized constant for the width of the ith central point.

As shown in **Figure 2**, the RBFNN structure is divided into three main parts: input unit, single hidden layer and output unit. The connection weight between the input layer and the hidden layer is set to a constant value of 1. In the core part of the model, the hidden layer has n neurons, and the Gaussian radial basis function is used as the activation function.

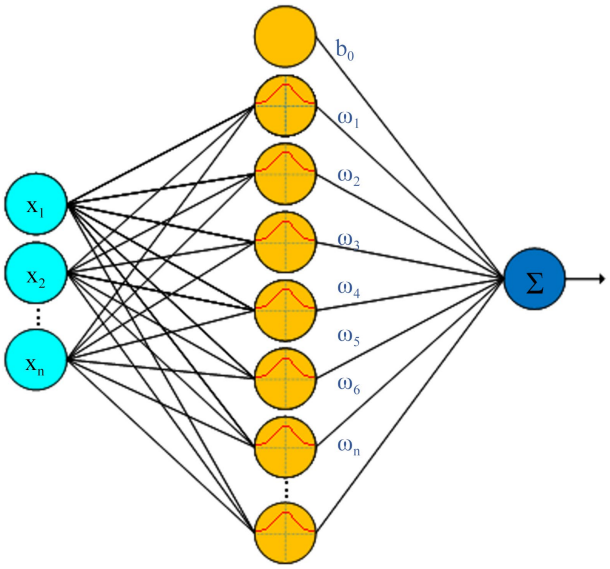

Figure 2. The structure of RBFNN.

The key issue of the learning algorithm for the RBFNN surrogate model is the reasonable value of the center parameter u_i of hidden-layer neurons. The K-means

clustering method is adopted to determine its center parameter u_i through self-organizing learning. The coefficient of determination R^2 is used to reflect the fitting degree of the RBFNN surrogate model to the observed values, and its calculation formula is shown as equation (4).

$$R^2 = 1 - \frac{\sum_{i=1}^{n}(y_i - \bar{y})^2}{\sum_{i=1}^{n}(\widehat{y_i} - \bar{y})^2} \tag{4}$$

Among them, y_i represents the predicted value of the surrogate model; $\widehat{y_i}$ represents the true value of the sample; $\bar{y}$ represents the sample mean.

Take the vehicle body vibration accelerations obtained from simulations under 1000 groups of different suspension parameter samples as predicted values, and the measured vehicle body vibration accelerations as true values. Based on equation (1), calculate the vertical and lateral vibration accelerations ρ_{zm} and ρ_{ym} between the predicted values and the true values. Use MATLAB software to construct vertical and lateral RBFNN surrogate models. Take the key parameters for vehicle body vertical vibration acceleration, *i.e.*, the vertical stiffness of the rubber pad, the vertical stiffness of the secondary spring, and the vertical stiffness of the elastic side bearing, as input variables, and ρ_{zm} as the output variable to construct the vertical RBFNN surrogate model. Take the calculated 1000 - group key parameters for vehicle body lateral vibration acceleration, including the vertical stiffness of the rubber pad, the lateral stiffness of the secondary spring, the vertical stiffness of the secondary spring, and the relative friction coefficient of the inclined wedge, as input variables, and ρ_{ym} as the output variable to construct the lateral RBFNN surrogate model.

5. The Analysis of the Results

Of the 1000 data sets, 70% were used as the training set and 30% as the validation set. By setting different initial cluster number *d*, the fitting degree and prediction accuracy of the surrogate model for 1000 sets of simulation data are verified with the determination coefficient R^2, and the R^2 of the training set and the validation set of the RBFNN surrogate model are observed, to determine the number of clusters *d*. Table 3 and Table 4 show the trend of R^2 value of vertical and horizontal surrogate models with the increase of cluster number *d*, respectively.

Table 3. The change trend of R^2 value of vertical surrogate model with the increase of cluster number *d*.

Serial numbers	Number of clusters *d*	Training set R^2 value	Validation set R^2 value
1	0	0.52	0.31
2	100	0.79	0.56
3	200	0.88	0.79
4	300	0.89	0.82

Continued

5	400	0.92	0.9
6	500	0.91	0.88
7	600	0.9	0.89
8	700	0.9	0.8
9	800	0.9	0.86
10	900	0.9	0.79

Table 4. The change trend of R^2 value of horizontal surrogate model with the increase of cluster number *d*.

Serial numbers	Number of clusters *d*	Training set R^2 value	Validation set R^2 value
1	0	0.42	0.3
2	100	0.69	0.46
3	200	0.87	0.69
4	300	0.8	0.7.2
5	400	0.92	0.9
6	500	0.91	0.89
7	600	0.9	0.89
8	700	0.9	0.85
9	800	0.9	0.85
10	900	0.9	0.84

As can be seen from **Table 3** and **Table 4**, when the number of clustering clusters is 400, the coefficient of determination R^2 of the training set and the test set reaches its maximum value, and both are greater than 0.9. When the coefficient of determination is above 0.8, the fitting effect of the surrogate model is considered good. Therefore, it can be concluded that the optimal number of clustering clusters is $d = 400$. At this time, the comparisons between ρ_{zm} and ρ_{ym} and the vertical predicted value ρ_{pzm} and the lateral predicted value ρ_{pym} of the surrogate model are shown in **Table 5** and **Table 6**.

Table 5. The comparison between predicted and actual values of vertical proxy model.

Serial numbers	Sample size	True Value ρ_{zm}	Predicted value ρ_{pzm}
1	10	0.74	0.7
2	15	0.65	0.62
3	20	0.71	0.68
4	25	0.63	0.62
5	30	0.73	0.73
6	35	0.65	0.65
7	40	0.78	0.77
8	45	0.79	0.8
9	50	0.71	0.74

Table 6. The comparison between the predicted value and the true value of the horizontal proxy model.

Serial numbers	Sample size	True Value ρ_{ym}	Predicted value ρ_{pym}
1	10	0.74	0.7
2	15	0.65	0.62
3	20	0.71	0.68
4	25	0.63	0.62
5	30	0.73	0.73
6	35	0.65	0.65
7	40	0.78	0.77
8	45	0.79	0.8
9	50	0.71	0.76

From Table 5 and Table 6, it can be seen that the error range between the simulation value and the predicted value of the vertical agent model is 0 - 0.03, and the error range between the simulation value and the predicted value of the horizontal agent model is 0 - 0.05, it shows that the accuracy of the surrogate model meets the requirements.

6. Conclusion

It is difficult to express the mathematical relationship between the key parameters to be optimized and the optimization objective by using the intuitive mathematical expression of the multi-body dynamics model of vehicle-track coupling, the RBFNN surrogate model between the key parameters to be suspended and the optimization target is built by MATLAB, and R^2 is used as an index to evaluate the accuracy of the surrogate model. The results show that the accuracy of the surrogate model meets the requirements.

Conflicts of Interest

The authors declare no conflicts of interest regarding the publication of this paper.

Fund

The research is funded by the Scientific research project of Hunan Provincial Department of Education, China (Wheel-Rail Adhesion Depth Modeling Based on Rail Surface Condition Identification, under Grant 22B1013).

References

[1] Yang, C.L., Huang, Y.H. and Ding, J. J. (2021) Influence of Geometric Parameters of Heavy Haul Track Curve on Wheel-Rail Coupling Dynamic Characteristics. *Journal of Transportation Engineering*, **21**, 215-227.

[2] Ma, H., Zhang, J., Zhang, J., Jin, T.T. and Song, C.Y. (2020) Influence of Full-Life Cycle Wheel Profile on the Contact Performance of Wheel and Standard Fixed Frog

in Heavy Haul Railway. *Shock and Vibration*, **2020**, 1-12. https://doi.org/10.1155/2020/8866692

[3] Li, J., Zuo, W., E, J., Zhang, Y., Li, Q., Sun, K., *et al.* (2022) Multi-Objective Optimization of Mini U-Channel Cold Plate with SiO_2 Nanofluid by RSM and NSGA-II. *Energy*, **242**, Article ID: 123039. https://doi.org/10.1016/j.energy.2021.123039

[4] Gribov, A. and Krivoruchko, K. (2020) Empirical Bayesian Kriging Implementation and Usage. *Science of The Total Environment*, **722**, Article ID: 137290. https://doi.org/10.1016/j.scitotenv.2020.137290

[5] Jie, H., Zheng, G., Zou, J., Xin, X. and Guo, L. (2020) Speed Regulation Based on Adaptive Control and RBFNN for PMSM Considering Parametric Uncertainty and Load Fluctuation. *IEEE Access*, **8**, 190147-190159. https://doi.org/10.1109/access.2020.3031969

[6] Sun, Y., Ding, S., Zhang, Z. and Jia, W. (2021) An Improved Grid Search Algorithm to Optimize SVR for Prediction. *Soft Computing*, **25**, 5633-5644. https://doi.org/10.1007/s00500-020-05560-w

[7] Hariri-Ardebili, M., Mahdavi, G., Abdollahi, A. and Amini, A. (2021) An RF-PCE Hybrid Surrogate Model for Sensitivity Analysis of Dams. *Water*, **13**, Article 302. https://doi.org/10.3390/w13030302

[8] Chen, J., Ji, X., Dey, *et al.* (2022) Intelligent Recognition of Pavement Distress Using Deep Convolutional Neural Network. *Journal of Fuzhou University* (*Natural Science Edition*), **50**, 530-536.